Landslides (2018) 15:2399–2412
DOI 10.1007/s10346-018-1056-3
Received: 6 March 2018
Accepted: 29 August 2018
Published online: 13 September 2018

Jian Chen · Wendy Zhou · Zhijiu Cui · Weichao Li · Saier Wu · Junxue Ma

Formation process of a large paleolandslide-dammed lake at Xuelongnang in the upper Jinsha River, SE Tibetan Plateau: constraints from OSL and ^{14}C dating

Abstract A large number of the landslide dams located on the major rivers at the southeastern margin of the Tibetan Plateau have been previously identified through remote sensing analysis and field investigations. The Xuelongnang paleolake was one of the lakes formed by these landslide dams in the upper Jinsha River, where the association of a relict landslide dam, lacustrine sediment, and outburst sediment is well preserved. This preservation provides an opportunity to better understand the formation, evolution, and longevity of a large landslide-dammed lake in the upper Jinsha River. It was inferred that the Xuelongnang dammed lake may have been formed by an earthquake-induced paleoavalanche. The surface area of the lake at its peak was estimated at 7.0×10^6 m^2, and the corresponding volume was approximately 3.1×10^8 m^3. Two outburst flood events were determined to have occurred during the life span of the lake. Based on the 18 ages obtained from optically stimulated luminescence (OSL) and carbon-14 (^{14}C) dating combined with stratigraphic sequences observed in the field, the paleolandslide-dammed lake was formed at approximately 2.1 ka and subsequently breached locally. The dammed lake was sustained for a period of some 900 years based on the chronological constraining. This study confirms that a major landslide-dammed lake can be sustained for at least hundreds of years and breached by several dam breaks in multiple periods, which contributed to the preservation of the knickpoints at millennial scale along the major rivers in the study area.

Keywords Paleolake · Optical dating · Formation process · Landslide dam

Introduction

Dammed lakes can form in many ways in nature (Costa and Schuster 1988). There are three geomorphologic regions within which these lakes were commonly found:

1. Alpine valley regions. The eastern or southeastern margin of the Tibetan Plateau (TP) of China is an example of such regions, where the rock avalanches, rock falls, or debris flow can block rivers (Dai et al. 2005; Zhang et al. 2011; Chen et al. 2013; Guo et al. 2016; Wu et al. 2016).
2. Alpine glacial regions. The southern side of the Tibetan Plateau and the Alpine glacial zones in South and North America are examples of such regions, where numerous ice-dammed or moraine-dammed lakes are well developed (Trauth and Strecker 1999; Korup and Montgomery 2008; Liu et al. 2015).
3. Volcanic belts. Dammed lakes may form in these regions due to lahars, pyroclastic flows, or volcanic debris avalanches which may block rivers (Waythomas 2001; Kataoka et al. 2008; Kataoka 2011).>

There have been numerous studies conducted regarding natural lakes and the corresponding dams (e.g., Clayton and Moran 1982; Korup and Montgomery 2008; Cui et al. 2009, 2012). These studies have focused on the site descriptions, hazard assessments, and fluvial responses and have included ice-, moraine-, landslide-, and volcano-dammed lakes.

These natural lakes and their dams are remarkably diverse in their formation, characteristics, and longevity (Costa and Schuster 1988). It has been found that the outburst and demise often occurred to the dammed lake after the backwater rose high enough to overflow the natural dam (Li et al. 1986; Dai et al. 2005). However, some of the dammed lakes were determined to have stably existed for long periods of time ranging from hundreds of years to thousands of years (Ermini and Casagli 2003; Korup and Tweed 2007). The water flows during the dam break outbursts achieved high magnitudes but had short durations (days to weeks) and were extremely erosive (Kehew and Lord 1986).

Large amounts of research data have been reported regarding the geomorphic and sedimentary consequences of the outburst flows on the proglacial outwash plains, the outlets of the caldera lakes, as well as in the moderate reliefs within high-latitude regions (Baker 1973; Costa 1983; Lord and Kehew 1987; Walder and Costa 1996; Cutler et al. 2002; Benn et al. 2006; Kataoka 2011). Furthermore, although geomorphic and sedimentary evidence of catastrophic outburst flows persists even in mountain belts subjected to high erosion rates, unequivocal reconstruction of the causes of damming and failure is not always straightforward (Korup and Tweed 2007).

A clear understanding of the processes including the formation and breaching of landslide-dammed lakes is crucial for hazard mitigation, as well as for the reconstruction of the previous events and landscape evolution (Korup 2002). Abundance of large-scale paleolandslides, along with their associated dammed lakes and relict dams, has been observed at the Batang-Zhongzan Reach along the upper Jinsha River valley, the southeastern margin of the TP (see Fig. 1). Some of the paleolandslides were dated in our previous work (Chen et al. 2013). The origin and evolution history of the major paleo-dammed lakes in the study area have drawn wide attention. It is suggested that the major paleo-dammed lake clusters may have formed in multiple periods through field investigation (Chen et al. 2013; Wang et al. 2014), despite the causes are still under debate. This study focuses on investigating the formation processes of the Xuelongnang major paleo-dammed lake, by examining the associations of the relict landslide dam, lacustrine sediment, and outburst sediment through field study in conjunction with optically stimulated luminescence (OSL) and ^{14}C dating.

The goals of this study include (1) characterizing the geomorphological and sedimentological features of the Xuelongnang paleo-dammed lake; (2) determining the formation and breaching time of the paleo-dammed lake, based on the constraints from

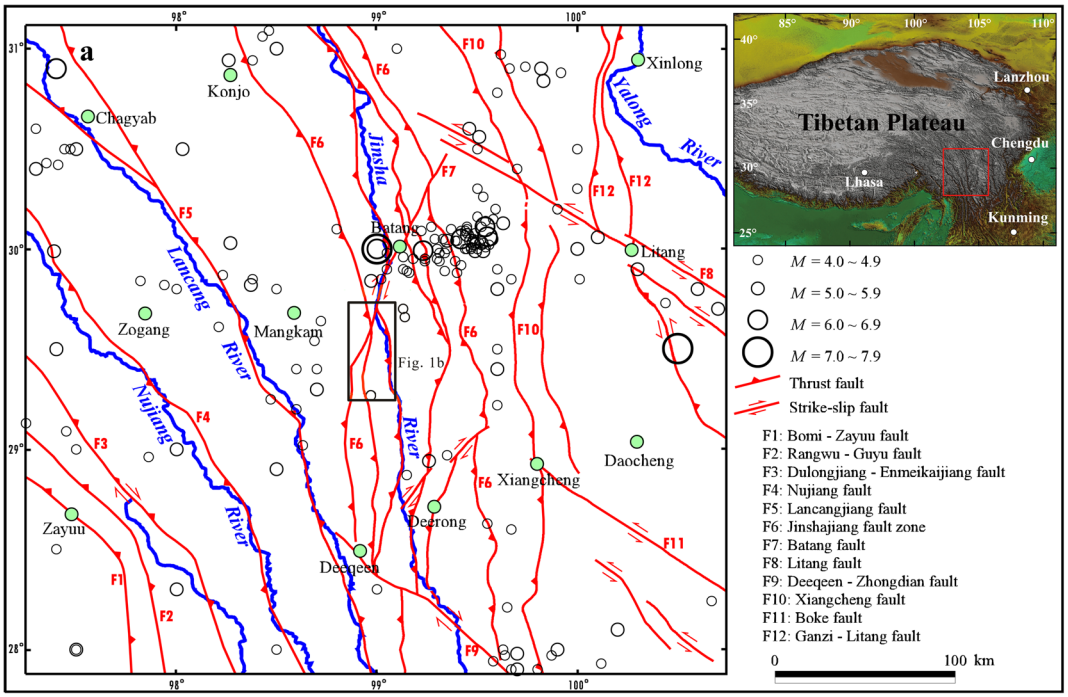

Fig. 1 Study area in the southeastern margin of the Tibetan Plateau. **a** Location map of the study area. **b** Geological map of the Xuelongnang Reach of the upper Jinsha River

OSL and ^{14}C dating; and (3) understanding the formation processes of the major landslide-dammed lake in the upper Jinsha River.

Regional setting

Since the late Cenozoic period, intense tectonic uplift results in deep incisions along the upper Jinsha River at the southeast margin of the TP (Burchfiel et al. 1995; Cui et al. 1996; Li and Fang 1998). This area is characterized by typical canyon landforms. The Xuelongnang-Wangdalong Reach has an average elevation greater than 2300 m and narrow valleys 100 to 200 m in width. The slopes in this area are steep, with the majority being greater than 30°.

On the valley floors, the climate is arid and hot due to the foehn effect. Annual average rainfall is less than 400 mm. The rainy season lasts from June to September (Chen et al. 2013). The annual average temperature is approximately 16 °C. However, the peak temperature can reach as high as 35 °C. Therefore, this area can be considered as having a subtropical dry-hot valley climate. The physical weathering is very strong, conditioned by the dry climate and large daily temperature variations, and consequently, soil erosion is very severe leading to sparse surface vegetation.

The lithologies of the exposed rock along the valley sides are mainly schist, marble, limestone, granite, and volcanic rocks, as illustrated in Fig. 1 (RGSTY (Regional Geological Survey Team of the Yunnan Bureau of Geology and Mineral Resources) 1982).

Two groups of major active faults are present within the study area: the Batang Fault (F1) and the Jinsha River Fault zone (F2). The Jinsha River Fault zone mainly contains four active faults: the Zengziding River Fault (F2-1), Zigasi-Deeqeen Fault (F2-2), Benxie-Dagaiding Fault (F2-3), and Xiongsong-Suwalong Fault (F2-4), as shown in (Fig. 1a). The faulted landforms and chronology allowed to estimate a strike-slip rate of the Jinsha River Fault zone of 6 to 7 mm/a and the vertical rate between 2 and 3 mm/a (Xu et al. 2005).

According to existing historic earthquake records (Wu and Cai 1992), strong seismic activities frequently occurred in the study area. As illustrated in Fig. 1, the active Xiongsong-Suwalong Fault runs through the eastern side of the Jinsha River valley. A number of major paleolandslides or paleolandside dams formed along the Xiongsong-Suwaong Fault zone (Chen et al. 2013).

Methodology

Sample collection

Several sections around the Xuelongnang landslide dam were selected for sampling for the purpose of OSL and ^{14}C dating. Deposits in these sections are comprised of lake sediments or outburst sediments. The lake sediment consists mainly of well-laminated clay and silt (locs. 1 to 6 and loc. 9 in Figs. 2 and 3). The outburst sediment consists of cobble, gravel, and sand (loc. 7 and loc. 8 in Figs. 2 and 3). The elevations were measured with a portable Trimble GeoExplorer 6000 Series (GPS). All of these sections are along the Upper Jinsha River, and the elevation of each section is shown in Fig. 2. The characteristics of the Xuelongnang paleolake before its draining are reconstructed through ArcGIS 10.0 based on the data from ASTER Global Digital Elevation Model (ASTER GDEM) version 2.

Sixteen luminescence samples and two ^{14}C samples at different levels of the sequences were collected. The OSL samples collected from the lacustrine and outburst sediments were determined to be silty-clay and fine sand, respectively. The two ^{14}C samples consist of organic matter or buried wood charcoal contained in the lake

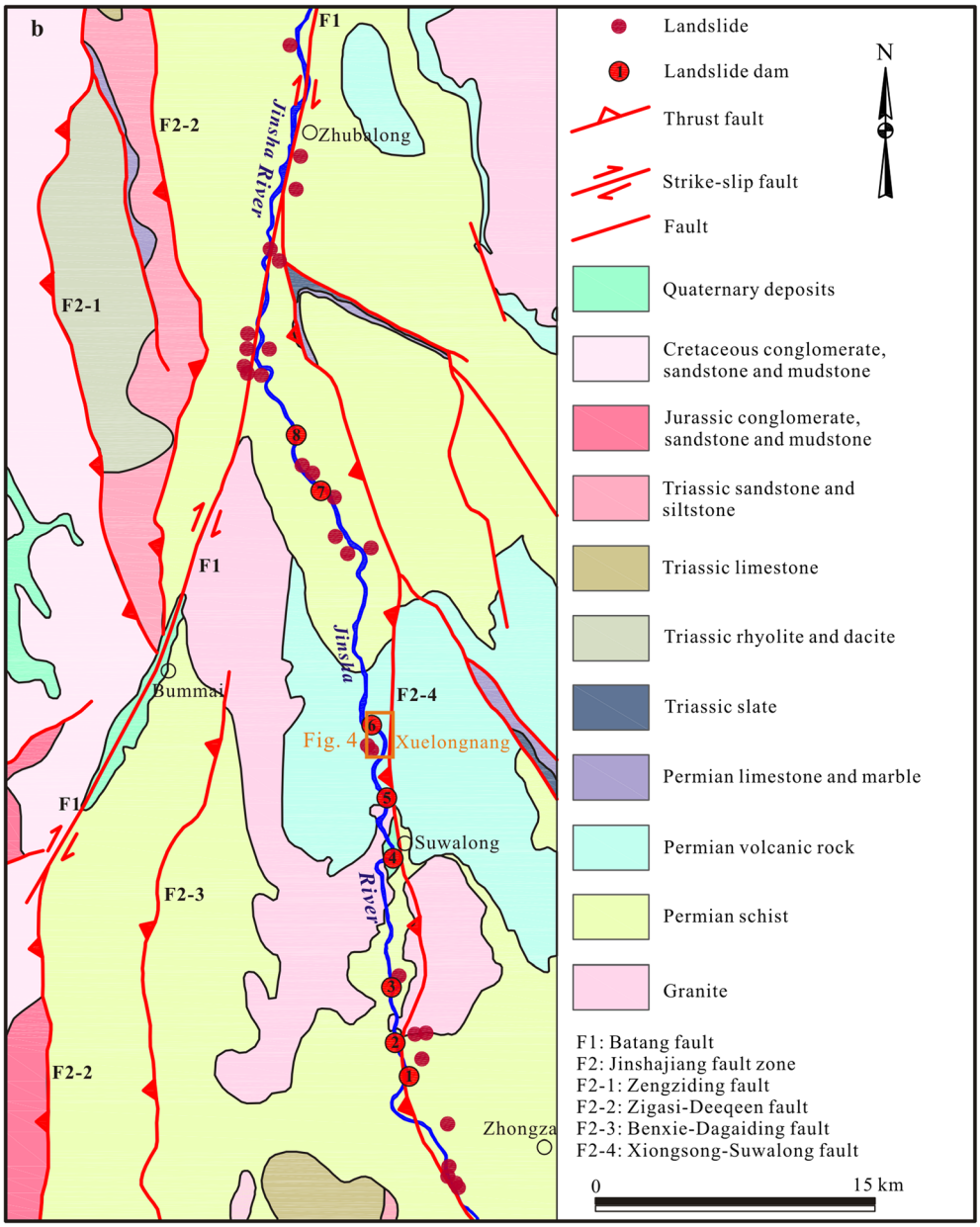

Fig. 1 (continued)

sediment. The concentration levels of uranium (U), thorium (Th), and potassium (K) for each sample were measured using a neutron activation analysis (NAA) and flame photometry, respectively, at the Chinese Atomic Energy Institute in Beijing. Cosmic gamma contribution was calculated following Prescott and Stephan (1982). The paleomoisture values were estimated based on the moisture content, with uncertainties of 5% for all of the samples.

Optically stimulated luminescence sample preparation and measurement

The OSL samples were taken from freshly cleaned profiles using steel tubes. The sample's exteriors were removed, and the middle portion was used to extract quartz for the equivalent dose (D_e) determination. The sample pretreatment and OSL measurements were performed under a subdued red light environment. Firstly, the raw ones were treated with 10% HCl and 30% H_2O_2 to remove carbonates and organic matter. Then, grains between 63~90 and 125~150 μm were selected by dry sieving and pretreated with sodium polytungstate heavy solution and 40% HF (for 2 h) to dissolve feldspars and clean quartz grains (Aitken 1998). The purity of quartz extract was tested using infrared-stimulated luminescence (IRSL). Contaminated samples were re-etched. All of the OSL measurements were performed using a RiSø TL/OSL-DA-15 in the Institute of Geology and Geophysics, Chinese Academy of Sciences, which was equipped with an internal $^{90}Sr/^{90}Y$ beta source and blue-light-emitting diodes (LEDs) (λ = 470 ± 20 nm). The luminescence signals were detected using a 9235QA photomultiplier tube, which was fitted with 7.5-mm-thick Hoya U-340 filters.

The optical measurements were performed after the samples were heated at a temperature of 260 °C for 10 s for the natural and

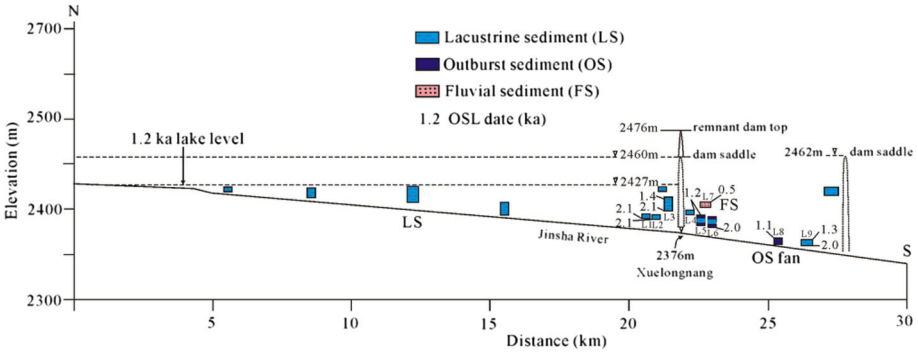

Fig. 2 Longitudinal river profile showing present-day elevation and location of all dating sections (locs. 1 to 9) is indicated

regenerative doses and after preheating at a temperature of 220 °C for 10 s for the test doses. The initial 2 s of 100 s of a shine-down curve was used for analysis. In this study, a single-aliquot regenerative-dose (SAR) protocol (Murray and Wintle 2000) method was used for D_e determination. This method had been previously successfully applied to dammed lake sediments (Chen et al. 2013; Wang et al. 2014; Guo et al. 2016). For each sample, 15–20 aliquots were measured using the SAR protocol. The mean of all SAR D_es is the final D_e for each sample (Murray and Wintle 2000).

The ^{14}C samples were measured using original bulk materials or buried wood charcoal in the accelerator mass spectrometry (AMS) ^{14}C laboratory at the Department of Archaeology, Peking University. The determination of the radioactive isotopes was accomplished using a method of a benzene liquid scintillation counter, and the averaged radiocarbon ages were performed using CALIB5.0.1 computer software developed by Washington University (Stuiver and Reimer 1993).

Results

Evidences for the damming and breaching

Generally speaking, the characteristic geomorphic features of a previously dammed lake can be summarized as follows: (1) the presence of a river with a large catchment area, which could potentially form a dammed lake following the introduction of a major damming body; (2) a breach rim formation, which is sometimes accompanied by thick lacustrine deposits in the upstream areas; and (3) pendant-shaped, band-shaped, or fan-shaped outburst landforms developed in the downstream areas (Scott and Gravlee 1968; Lord and Kehew 1987; Reneau and Dethier 1996; Benn et al. 2006; Kataoka 2011; Chen et al. 2013; Van Gorp et al. 2013). In the Xuelongnang Reach of the upper Jinsha River, all the three geomorphic features, i.e., relicts of a landslide dam and upstream lacustrine deposits, as well as downstream pendant- or band-shaped outburst accumulation landforms, have been observed in the field. These features indicate that a major landslide-dammed event had occurred and that the dam subsequently breached (Fig. 4). These geologic and geomorphologic characteristics will be described in the subsequent subsections.

Relict landslide dam

A large paleolandslide was recognized along the Xuelongnang Valley, located on the western bank of the upper Jinsha River, within the territory of Mangkang County, Tibet, during a field excursion. The relict landslide dam, located on the western bank of Jinsha River, is approximately 700 m long and 600 m wide and has a dam-front thickness of approximately 84 m, with an estimated landslide volume of ~ 2.3×10^7 m^3 through field investigation (Fig. 5). The landslide dam materials consist of diamicton, ranging from sand, gravel to boulders (Fig. 6a, b). At this location, the boulders are poorly sorted and unstratified beige-colored schist, with maximum diameters of up to 4 m. Another diamicton accumulation overlays the slope of the bedrock on the eastern bank (Fig. 6c). The top of the diamicton deposit is approximately 100 m above the current water level of the Jinsha River and approximately of 1.5×10^4 m^3 in volume. The deposit materials are mainly clast-supported boulder gravel consisting of beige-colored schist, which are the same as the landslide deposit materials on the western bank. These evidences suggest that all of these accumulations of the landslide deposit blocked the river at once. The river reach, where the landslide relict is exposed, is very narrow with a width of 80 m, which makes it easy for rapids or cascades to form. Additionally, there are many boulders accumulated on the river's gravel beach, with a maximum diameter of 6 m. These were found to be poorly sorted and angularly shaped, which also suggests their association with the relict accumulation of the dam following the breakdown of a landslide dam.

Lacustrine deposits in the upstream area

Within the study area, thick lacustrine silty-clay deposits with well-developed bedding were found to overlay the landslide deposits (Fig. 6a) or fluvial terraces on the western bank (Fig. 7a). Silty-clay layers (lacustrine facies) with horizontal bedding development were observed, approximately 200 m upriver from the relict landslide deposit along the eastern river bank. The exposed thicknesses of lacustrine deposit range from 3 to 5 m, and the top elevation is at approximately 2427 m, as shown in Fig. 7b. Soft-sediment deformation structures (SSDS) were observed in the exposed lake sediment layer located at the bottom of the Xuelongnang Valley (Fig. 6d). A 25-cm-thick silty-clay layer is characterized by the presence of curvilinear laminae and folds, along with a mixing of clastics draped by broken silty-clay laminae. The mixed clastics consisting of sand is exposed as inclined dykes. The silty-clay layer is underlaid by a 20-cm-thick brownish fine sand horizon. The material of the mixed clastics appears to have originated from the underlying sand horizon.

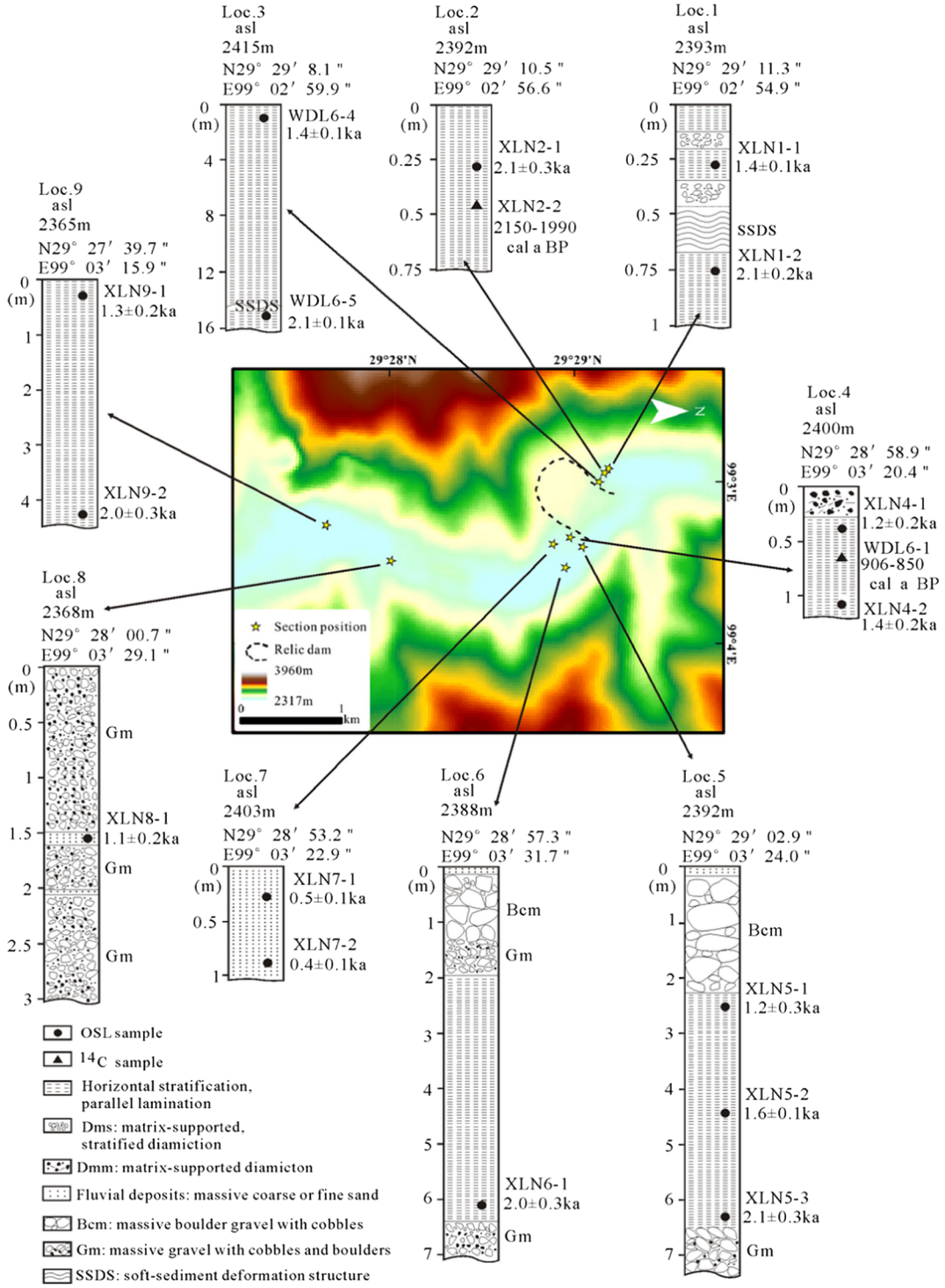

Fig. 3 Columnar sections showing the stratigraphy and dating ages of samples

The lacustrine deposits were observed from the landslide dam to as far as approximately 16 km upriver along the banks of the Jinsha River. The lacustrine deposits form platform-shaped terrain and almost continuously distribute along the banks on both sides of the Jinsha River, as well as overlay on the level-1 fluvial terrace (T1) (Fig. 7a). The thickness of lacustrine deposits can reach up to 16 m in this area. The dimensions of the lacustrine sediments allow us to infer an elongated narrow strip shape of a paleolake. It was observed that the thickness of the lacustrine deposit is only 3 m at the end of the backwater lake area. The top elevation of the lacustrine deposits here is at approximately 2425 m. The thick lacustrine deposits develop with distinct

Fig. 4 Map showing the locations of the Xuelongnang landslide dam, lake deposits, and outburst deposits

horizontal bedding and extend upriver along the banks of the Jinsha River. The thicknesses were found to gradually become thinner, but the top elevation of the lacustrine deposits basically remained the same.

Outburst bar deposits in the downstream area

An abundance of diamicton accumulation (Flint et al. 1960; Cui 1988; Cui et al. 2013) was found to be distributed along both sides of the river between the reaches from the Xulongnang landslide dam to as far as 3.5 km downstream. Some of this relict accumulation was exposed on the slope's bedrock appearing as "river terraces," while others were exposed on both sides of the river bed appearing as a high "floodplain," showing as "pendant-shaped" or "band-shaped" in bird's eye view.

The relict outburst diamicton accumulation was recognized at three different levels of elevation. The outburst deposit at the highest elevation was found to be exposed above the slope's bedrock on the east bank, with a top elevation of approximately 2420 or 44 m above the present river channel. The second deposit level was located on the downriver side of the landslide dam on the west bank (Fig. 8a) and had an elevation of approximately 2394 m at the top. Two sets of outburst diamicton layers are identified along the vertical profiles of the second deposit level. It was estimated that the thickness of the upper diamicton layer was

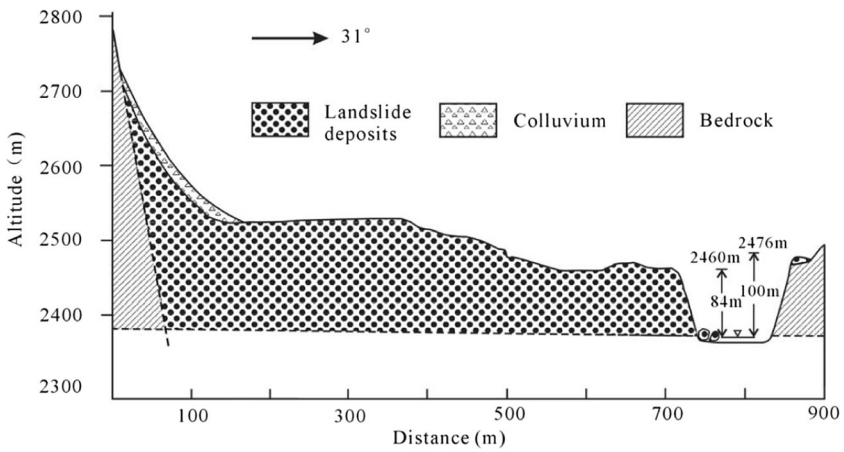

Fig. 5 Spillway cross section of the Xuelongnang landslide dam

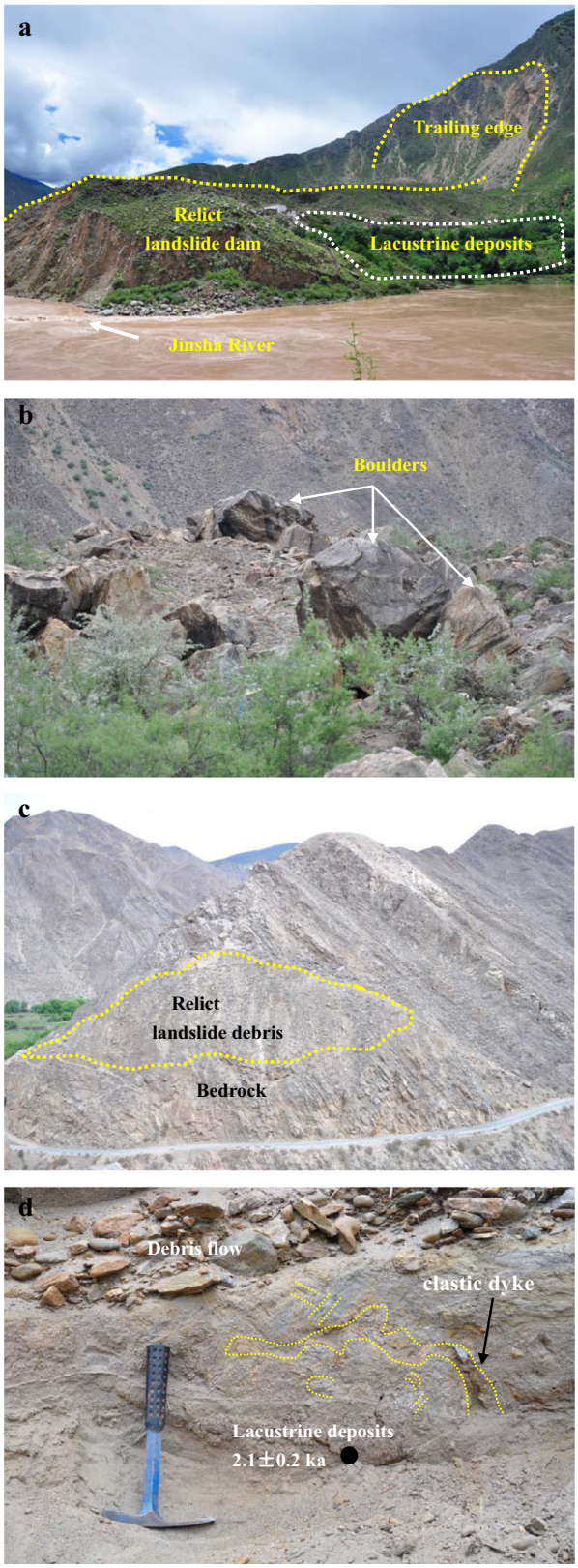

Fig. 6 Photographs taken in the Xuelongnang Valley. **a** Relict landslide dam and lacustrine deposits on the western bank of the Jinsha River. **b** Boulders accumulated on the top of dam-front of residual landslide dam. **c** Relict landslide debris overlying the bedrock on the eastern bank of the Jinsha River. **d** Clastic dyke developed at the bottom of the upstream lacustrine sediments

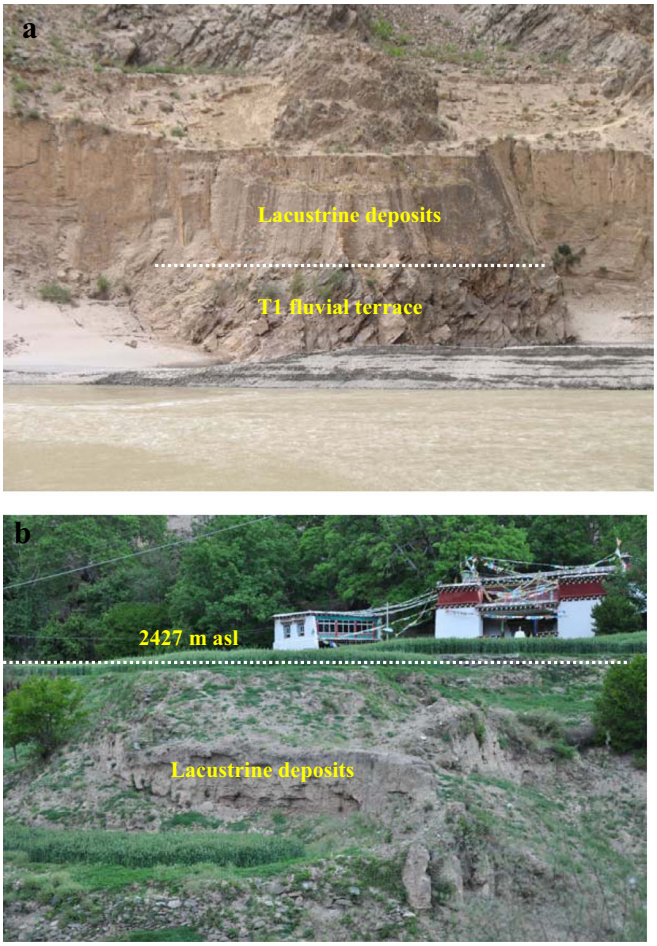

Fig. 7 Lacustrine deposits in the upstream area. **a** Lacustrine deposits with parallel bedding overlying the T1 fluvial terrace at the western bank. **b** Well-developed lacustrine deposits about 150 m upriver from the landslide dam at the eastern bank

about 4 m, while the thickness of the lower diamicton layer was approximately 11 m. The lacustrine strata downriver of the dam were deposited between two outburst deposits, with a thickness of approximately 4.5 m, and were overlaying the lower outburst diamicton layers (outburst deposit I) (Figs. 6c and 8b, loc. 5). Two kinds of typical sedimentary structures were identified in the outburst deposits: gravel support-stacked structure (Fig. 8d) and rhythmite-interbedded structure (Fig. 8e). The lacustrine deposits downriver of the dam locally show a clear cross-lamination structure about 4.5 m thick. The outburst deposit at the lowest elevation was observed on both sides of the current riverbed, and an imbricated structure can be clearly seen in this set of deposit (Fig. 8f). The top elevation of this deposit was approximately about 2373 m or only 2 to 5 m above the current level of the river surface.

From the viewpoint of accumulation positions of these diamicton deposits, no large tributary stream or debris-flow gully was found around the deposits, which indicated that the diamicton deposits are sourced from the main channel. The diamicton accumulations consist exclusively of beige-colored schist, which is consistent with the lithology of the clastics of the landslide dam. These findings indicated that the accumulation of the landslide dam was the main source of the downstream diamicton

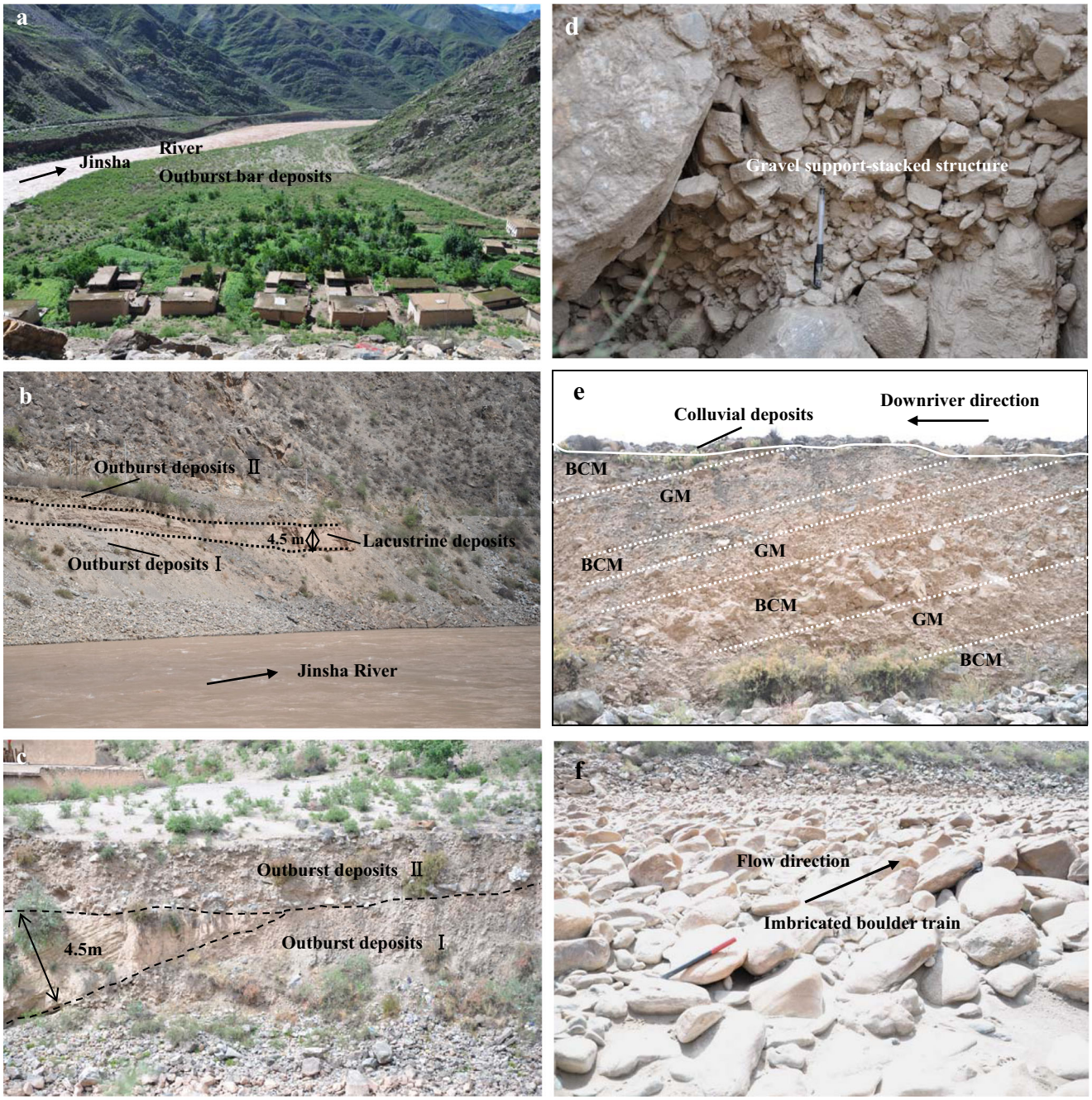

Fig. 8 Photographs of the outburst bar deposits (no. 1) downriver from the Xulongnang landslide dam. **a** Pendant shape of outburst bar deposits (no. 1) in plan view and view to downriver. **b** Two sets of outburst deposits with a set of lacustrine layer ~ 4 m in thickness intercalated developed in the eastern blank, showing two outburst events. **c** Two sets of outburst deposits with a set of lacustrine layer intercalated developed in the western blank. **d** Clear gravel support-stacked structure within outburst deposits. **e** Rhythmite-interbedded structure composed of boulder facies (BCM facies) and clast-supported cobble and boulder gravel facies (GM). **f** Downstream of longitudinal midchannel bar (no. 2), with sorted boulders ~ 0.2 m in diameter. Note boulder imbrication (flow left to right)

accumulations. Additionally, the diamicton accumulations were only found in the downstream of the landslide-dam relict, and this evidence supports the interpretation that these are products of landslide-dam outburst.

Dating results

Figure 9 details the preheat plateaus for quartz, shine-down curve, radial plot, growth curve, and distribution of equivalent dose (D_e) of sample XLN4-1. Figure 9b shows that the OSL signals decrease very quickly during the first 2 s of stimulation, indicating that the OSL signal is dominated by the fast component. The distribution of D_e (sample XLN4-1) approximates a positive skewed distribution shape, indicating that the sample was being relatively well-bleached.

The OSL dates are listed in Table 1 and are also shown in Fig. 3. The calibrated ages for the ^{14}C samples are listed in Table 2.

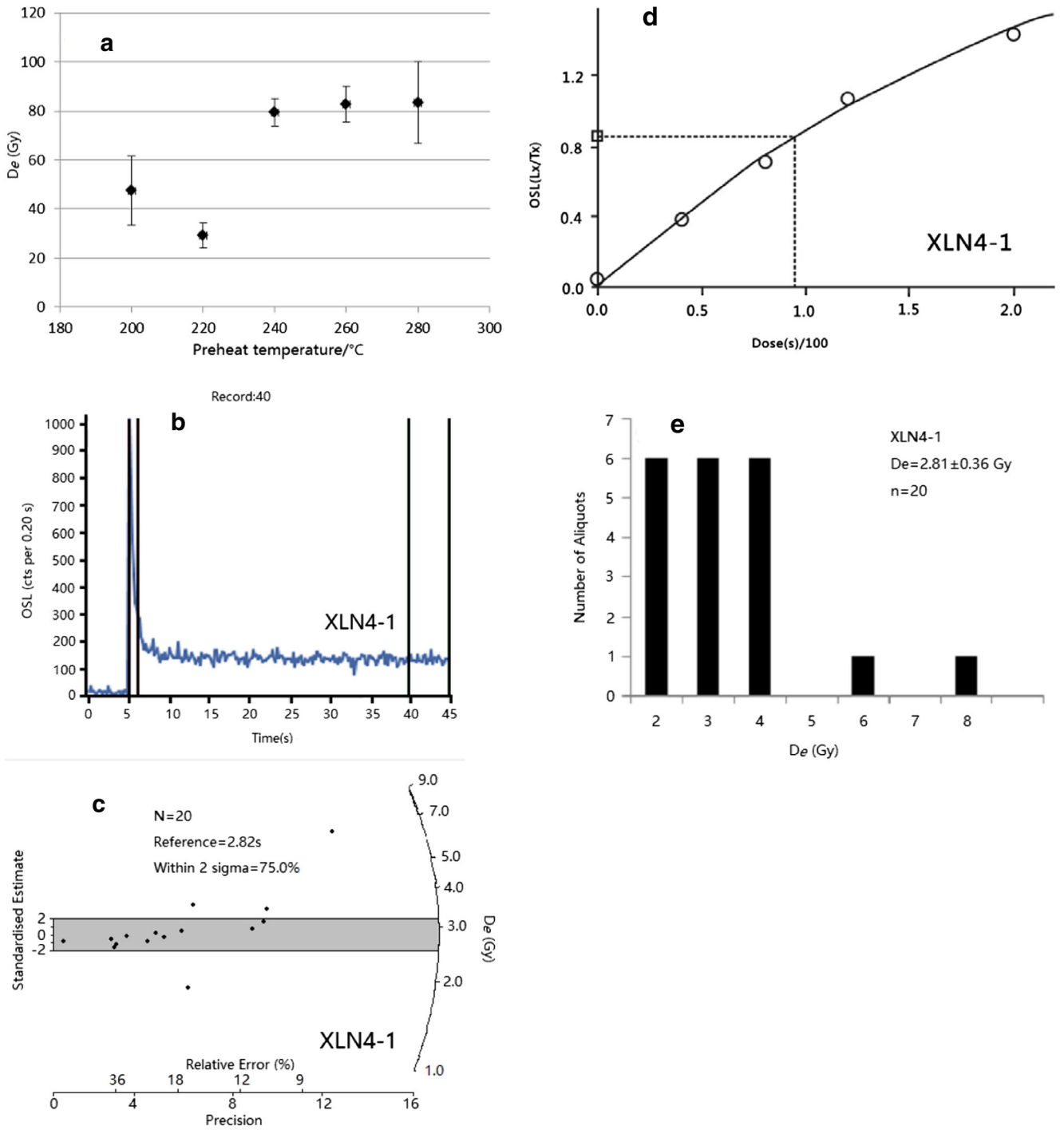

Fig. 9 OSL data: **a** preheat plateaus for quartz, **b** shine-down curves, **c** radial plot, **d** growth curves, and **e** distribution of equivalent dose (D_e) of sample XLN4-1

Discussion

Timing of dam formation and breaching

In this study, it was confirmed that this particular set of lacustrine deposits upriver of the landslide dam was in fact a set of landslide-dammed lake deposits through correlating the spatial relationship between the locations of the landslide mass and lacustrine deposits and the sedimentary features of the observed lacustrine deposits. These findings revealed that a large rock avalanche had dammed the Jinsha River in the study area once upon a time.

It is known that a landslide-dammed lake may last for as short as several minutes, or as long as several thousand years depending on many factors (Costa and Schuster 1988; Ermini and Casagli 2003). These factors include (1) the volume, size, shape, and sorting of the blockage material; (2) rates of seepage through the blockage; and (3) rates of the sediment and water flow into the

Table 1 OSL dating results of samples

No.	Section	U (ppm)	Th (ppm)	K (%)	D_e (Gy)	Dose rate (Gy/ka)	Water content (%)	Age (ka)
XLN1-1	Loc. 1	2.05	10.2	2.0	4.8 ± 0.4	3.46 ± 0.17	0.8	1.4 ± 0.1
XLN1-2	Loc. 1	1.25	8.1	1.59	5.6 ± 0.5	2.72 ± 0.14	0.27	2.1 ± 0.2
XLN2-1	Loc. 2	2.24	8.75	1.35	5.84 ± 0.70	2.78 ± 0.13	0.26	2.1 ± 0.3
WDL6-4[a]	Loc. 3	2.66	10.9	1.63	4.30 ± 0.33	3.04 ± 0.05	3.6	1.4 ± 0.1
WDL6-5	Loc. 3	2.13	11.55	2.92	10.46 ± 0.11	4.98 ± 0.20	2.0	2.1 ± 0.1
XLN4-1	Loc. 4	1.98	6.31	1.15	2.81 ± 0.36	2.34 ± 0.11	0.18	1.2 ± 0.2
XLN4-2	Loc. 4	1.41	7.49	1.2	3.33 ± 0.35	2.32 ± 0.11	0.2	1.4 ± 0.2
XLN5-1	Loc. 5	1.39	6.89	1.13	2.73 ± 0.60	2.22 ± 0.10	0.23	1.2 ± 0.3
XLN5-2	Loc. 5	1.48	7.25	1.18	3.69 ± 0.30	2.33 ± 0.11	0.18	1.6 ± 0.1
XLN5-3	Loc. 5	1.58	8.07	1.18	5.00 ± 0.73	2.34 ± 0.11	0.26	2.1 ± 0.3
XLN6-1	Loc. 6	1.31	6.95	1.47	4.9 ± 0.6	2.4 ± 0.13	0.33	2.0 ± 0.3
XLN7-1	Loc. 7	1.7	7.66	1.33	1.32 ± 0.36	2.55 ± 0.12	0.3	0.5 ± 0.1
XLN7-2	Loc. 7	1.83	8.88	1.37	1.01 ± 0.14	2.69 ± 0.13	0.25	0.4 ± 0.1
XLN8-1	Loc. 8	1.2	6.4	1.49	2.6 ± 0.4	2.43 ± 0.13	1.6	1.1 ± 0.2
XLN9-1	Loc. 9	2.97	7.41	1.29	3.69 ± 0.66	2.79 ± 0.12	0.55	1.3 ± 0.2
XLN9-2	Loc. 9	1.6	6.75	1.27	4.84 ± 0.68	2.39 ± 0.11	0.26	2.0 ± 0.3

[a] From Chen et al. (2013)

newly formed lake (Costa and Schuster 1988). Landslide dams commonly fail through overtopping, followed by breaching from erosion caused by the overflowing water. In most of the documented cases, dam breaches are caused by the fluvial erosions of the landslide material when the head-cutting initiates at the toe of the dam and progressively moves upstream to the lake (Costa and Schuster 1988; Ermini and Casagli 2003). Once the head-cutting reaches the lake, breaching occurs.

The results from OSL and ^{14}C dating in this study have revealed that the ages of the OSL samples at the bottom of lacustrine sections (locs. 1, 2, and 3), at the upstream of the residual landslide dam, are 2.1 ± 0.2, 2.1 ± 0.3, and 2.1 ± 0.1 ka, respectively. The age of the ^{14}C sample XLN2-2 at the bottom of loc. 2 section is 2150–1990 cal a BP, which is in good agreement with the OSL ages (Fig. 3). These data confirm that the paleo-dammed lake formed at approximately 2.1 ka.

Within the area of interest, lacustrine sediment platforms were also observed downstream of the residual Xuelongnang landslide dam (see locs. 5, 6, and 9). Chen et al. (2013) describe two other large, ancient landslide dams near the study site along the reach from Wangdalong to Xuelongnang in the upper Jinsha River formed around 1900 ± 60 a BP, which were inferred to be associated with a large paleoearthquake by a previous study. Therefore, this study considered that the reason for the formation of the lacustrine sediment downstream of this dam was that previously another landslide dam downstream blocked the river and formed another dammed lake later. The strata of the two sections (locs. 5 and 6) from top to bottom include outburst sediment, lacustrine sediment, and outburst sediment, sequentially (Fig. 8b, c). The intercalated lacustrine layer is approximately 4.5 m in thickness and extends to at least 800 m in length. The combination of stratigraphic sequence and age dating results suggests that there had been at least two outburst flood events in the Xuelongnang area. The ages of OSL samples, XLN5-3 and XLN6-1, at the bottom of the lacustrine sections (locs. 5 and 6) are 2.1 ± 0.3 and 2.0 ± 0.3 ka, respectively, which indicate that the first outburst flood event occurred at least 2.1 ± 0.3 ka. Samples XLN7-1 and XLN7-2 were collected from the top of the fluvial sediment (consists of gray coarse sand or fine sand, nonlaminated) in loc. 7 section (Fig. 3) with the OSL ages of 0.5 ± 0.1 and 0.4 ± 0.1 ka, respectively. These indicate that the dammed lake breached, new river channels formed, and a flood event occurred at least 0.5 ka.

Table 2 ^{14}C dating results of lake deposit samples

No.	Section	Material	^{14}C age[a] (a BP)	Calibrated age (2σ)[b] (cal a BP)
XLN2-2	Loc. 2	Black mud	2100 ± 25	(2150–1990) 2070
WDL6-1[c]	Loc. 4	Wood charcoal	900 ± 60	(906–850) 878

[a] Averaged radiocarbon ages were obtained using the developed computer program CALIB 5.0.1 (Stuiver and Reimer 1993) with an error multiplier of 2.0 for the original analyses

[b] Calibrated ages used the developed computer program 5.0.1 (Stuiver and Reimer 1993); ages are 2σ range

[c] From Chen et al. (2013)

The ages of four OSL samples collected at the top of four lacustrine sections range from 1.2 ± 0.2 to 1.4 ± 0.2 ka (Fig. 3), which indicate that the final outburst event occurred after 1.2 ka due to possible overtopping dam break, resulting in the termination of the Xuelongnang paleo-dammed lake. Therefore, it can be deduced that the Xuelongnang paleo-dammed lake may have formed at approximately 2.1 ka, and subsequently, the landslide dam breached locally. The landslide dam was then sustained for a long period of time. Finally, the dam breached completely, and the Xuelongnang dammed lake ended at approximately 1.2 ka. This study confirms that one long-standing landslide-dammed lake had been sustained for some 900 years in the upper Jinsha River valley, which indicates that a major landslide-dammed lake may be capable of remaining stable for a duration at the millennial scale (Costa and Schuster 1988; Hermanns et al. 2004; Korup and Tweed 2007; Hanson et al. 2012). Therefore, damming events may have made important contributions to the preservation of the knickpoints along the major rivers at the southeastern margin of the TP (Korup and Montgomery 2008).

Scale of the landslide-dammed lake

The lake sediments on the upstream side of the landslide dam were all found to be between 2390 and 2430 m asl in elevation (see Fig. 3). These elevations are below the top of the residual landslide dam surface elevation (2460 m asl) at Xuelongnang Village. The ages of lake sediments at the different elevations were all found to be similar (Fig. 10), which suggest that there was only one stage of the paleo-dammed lake in the Xuelongnang gorge. The surface elevation of the original paleo-dammed lake was about 2460 m asl. The surface area of the lake at its peak was estimated at 7.0×10^6 m^2, and the corresponding volume was approximately 3.1×10^8 m^3 (Fig. 11).

Triggering mechanism of the landslide-dammed lake

Clastic dykes, curvilinear laminae, and folds were widely discovered during this study in the upstream lake sediment within the extent of ~ 16 km. The age of sample no. XLN1-2, collected from the lake sediment underlying the SSDS layer in loc. 1 section, was confirmed to be 2.1 ± 0.1 ka based on the OSL analyses (Fig. 8). Clastic dykes are considered to be associated with underlying fine sand horizons. These features can be produced by earthquake-induced elevated fluid pressure or weight of overburden. Such pressure can be released through the upward flow of fluid, liquefaction, and fluidization (Lowe 1975; Mills 1983; Obermeier 1996; Owen 1996). The lacustrine deposits downriver of the dam has a cross-lamination structure in thick layers (4.5 m thick), also indicating that the lacustrine deposits may have experienced intense soft-sediment deformation subsequently. The presence of more than one type of SSDS, along with widely distributed thick deformation layers (thickness > 20 cm), and geological settings with frequent earthquake occurrences suggest that the genesis of these features is predominantly due to paleoseismic events.

Landslide is slope instability processes, which are the product of local geomorphic, hydrologic, and geologic conditions. The modification of these conditions can be caused by geodynamic processes, vegetation, land use practices, and human activities, as well as the frequency and intensity of rainfall and seismicity (Soeters and Van Westen 1996). According to previous studies (Keefer 1984; Schuster et al. 1996; Reid and Page 2003; Wilford et al. 2004; Korup et al. 2012; Regmi et al. 2014), rainfall, earthquakes, and fluvial incision are the three principal mechanisms inducing landslides. Several studies have identified characteristics of coseismic landslides, particularly those caused by large-scale earthquakes (Keefer 1984; Jibson et al. 1994; Khazai and Sitar 2004).

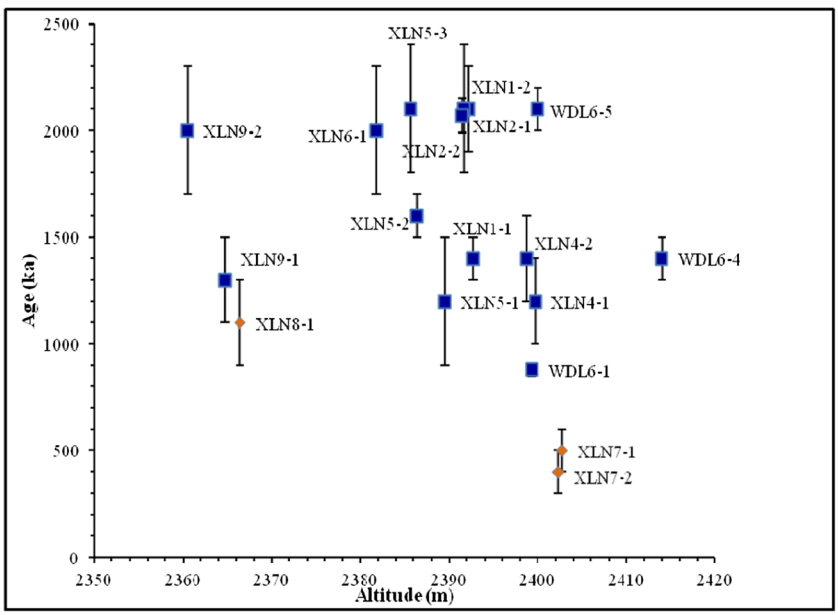

Fig. 10 All OSL and ^{14}C dates from around the Xuelongnang landslide dam. The errors of ages are also shown. Blue square symbol denotes the lacustrine deposits dated and orange diamond symbol denotes the fluvial deposits dated

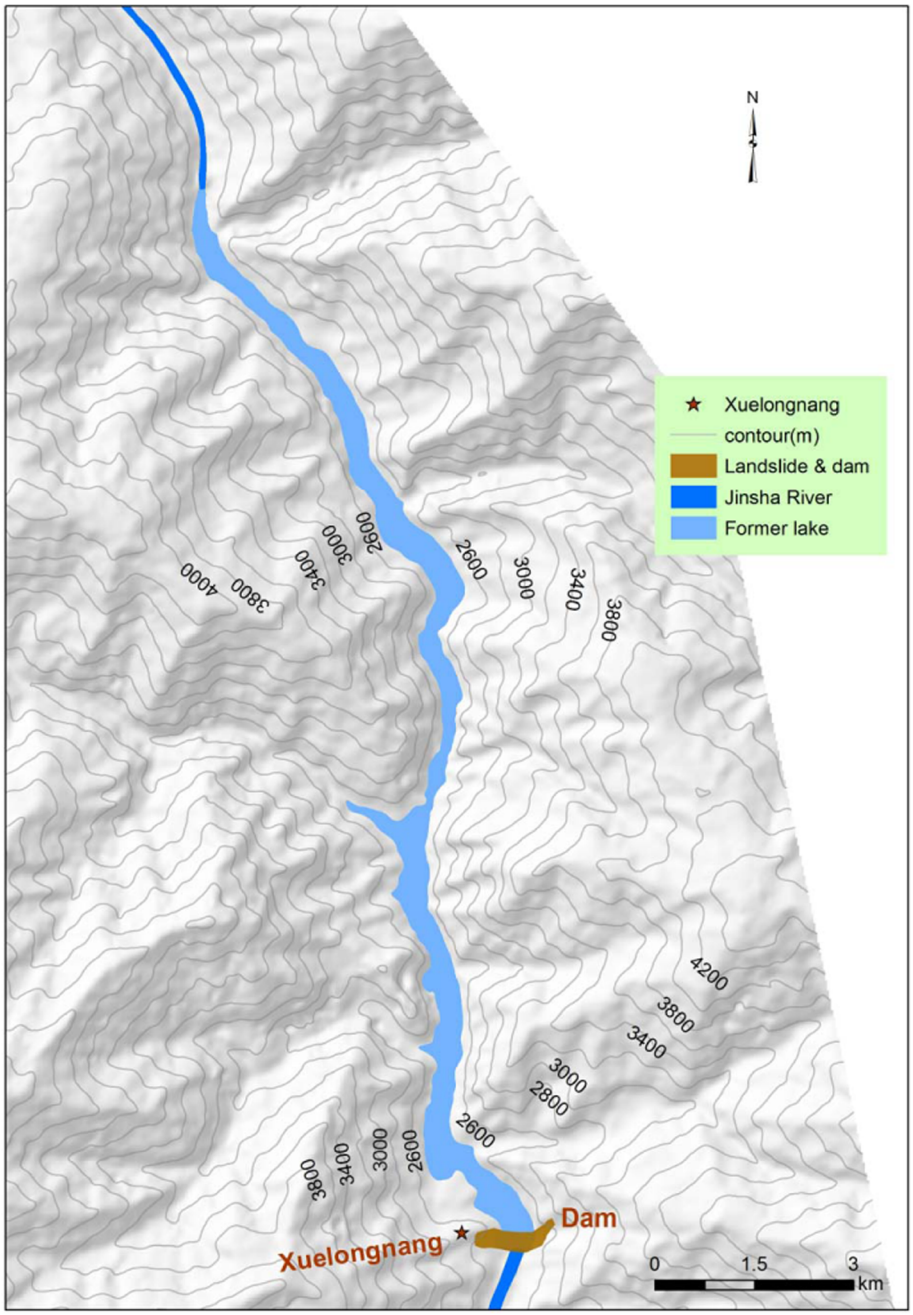

Fig. 11 Map showing the reconstructed lake (2460 m asl) behind the landslide dam

In regard to the triggering mechanism of the paleolandslide-dammed lake, the conclusion drawn through this study suggests that most of the landslides were triggered by earthquakes based on the following rationales.

On one hand, Xuelongnang Reach is located in a semiarid climate, with an average annual rainfall of less than 400 mm. The paleoclimate records and modern meteorological observations show that the water vapors in the Qinghai-Tibet Plateau and its adjacent areas mainly originated from the Indian Ocean (Hodell et al. 1999; Chen et al. 2008). The southwest monsoons have important influences on the climate in the study area. In the upstream section of the Jinsha River, the climate was relatively warm and humid during the 11 to 5 ka BP. After approximately 3.8 ka BP, however, the temperature and precipitation showed noticeable decreases. This change was attributed to weakened southwestern monsoons (Hodell et al. 1999). The exposed rocks on both sides of the Xuelongnang area are mainly hard volcanic rock intercalated with schist, which are found to be well cemented and stable under natural conditions. During the late Holocene period, the Xuelongnang Valley was dominantly characterized by minimal rainfall and a dry climate. Therefore, it could be inferred that it is less likely that any large dam-forming landslides (rock avalanches) be induced by rainfall or fluvial incision in this dry valley area.

On the other hand, Xuelongnang Reach is located in a well-known tectonically active region, which has the potential geological conditions for strong earthquakes (Wu and Cai 1992; Wen et al. 2008). The Xiongsong-Suwalong Fault (F2-4) is the main fault among the Jinsha River active fault zones, and it runs through this area along the Jinsha River valley. Multiple historical seismic events with magnitude of ≥ 6 since 1722 occurred in the study area based on historic seismic records (Wang et al. 2014). In the study area, the Xuelongnang paleolandslide dam is about 2 km away to the east side of the Xionsong-Suwalong active fault. According to our previous work (Chen et al. 2013), a number of major paleolandslides and paleolandslide dams were developed on both sides of the valleys within the Xuelongnang-Wangdalong Reach and linearly concentrated along the Xiongsong-Suwalong active fault. This study found that the existing sedimentology and chronology evidences are in agreement with the results of previous studies (Chen et al. 2013; Wang et al. 2014), that is, paleoearthquakes might have occurred in the Xuelongnang-Wangdalong Reach, along the upstream section of the Jinsha River during the late Holocene period. Through extensive examinations of the paleoearthquake, paleoclimate, and landslide chronology, we can infer that the Xuelongnang paleolandslide-dammed lake is considered to have been the result of a large rock avalanche which was triggered by a paleoearthquake.

Conclusions

Detailed field investigation and field sample OSL and ^{14}C dating were conducted for better understanding the formation process of the Xuelongnang paleolake in the upper Jinsha River valley, southeastern Tibetan Plateau. The OSL and ^{14}C dating were carried out to obtain the ages associated with major events during the life span of the paleolake. The integrated utilization of data obtained during the field investigation and sample age measurements revealed that the large paleolake formed in the Xuelongnang Reach during the late Holocene period.

We conclude that the Xuelongnang paleolake is due to a large rock avalanche which was triggered by one strong paleoearthquake. The Xuelongnang paleorock avalanche ran out far enough to cross the river and subsequently formed the landslide-dammed lake. There were at least two outburst flood events during the life span of the Xuelongnang landslide-dammed lake, which was formed at approximately 2.1 ka and subsequently breached locally at one time. The dammed lake was then sustained for a period of some 900 years and finally deceased at approximately 1.2 ka. The surface area of the lake at its peak was estimated 7.0×10^6 m^2, and the corresponding volume was approximately 3.1×10^8 m^3. Our study supported that it was possible for a major landslide-dammed lake to be sustained for a time period of hundreds of years, and breached by several dam breaks in multiple events. The longevity of large paleolandslide-dammed lakes may have contributed to the preservation of knickpoints along the major rivers at millennial scale at the southeastern margin of the Tibetan Plateau.

Funding informationThis study was supported by the National Natural Science Foundation of China (grants nos. 41571012 and 41230743), the Open Research Fund of the State Key Laboratory of Simulation and Regulation of Water Cycles in River Basins (grant no. IWHR-SKL-201507), and the Fundamental Research Funds for the Central Universities (grant no. 2652015060).

References

Aitken MJ (1998) An introduction to optical dating. Academic, London
Baker VR (1973) Paleohydrology and sedimentology of Lake Missoula flooding in eastern Washington. Geol Soc Am, Spec Pap 144:79
Benn DI, Owen LA, Finkel RC, Clemments S (2006) Pleistocene lake outburst floods and fan formation along the eastern Sierra Nevada, California: implications for the interpretation of intermontane lacustrine record. Quat Sci Rev 25:2729–2748
Burchfiel BC, Chen ZL, Liu YP, Royden LH (1995) Tectonics of the Longmen Shan and adjacent regions, central China. Int Geol Rev 37(8):661–735
Chen J, Dai FC, Yao X (2008) Holocene debris-flow deposits and their implications on climate in the upper Jinsha River valley, China. Geomorphology 93:493–500
Chen J, Dai FC, Lv TY, Cui ZJ (2013) Holocene landslide–dammed lake deposits in the Upper Jinsha River, SE Tibetan Plateau and their ages. Quat Int 298:107–113
Clayton L, Moran SR (1982) Chronology of late Wisconsin glaciation in middle North America. Quat Sci Rev 1:55–82
Costa JE (1983) Paleohydraulic reconstruction of flash–flood peaks from boulder deposits in the Colorado Front Range. Geol Soc Am Bull 94:986–1004
Costa JE, Schuster RL (1988) The formation and failure of natural dams. Geol Soc Am Bull 100(7):1054–1068
Cui ZJ (1988) Discussion on the discrimination principle and symbol of origin on the diamicton and diamictite. Geol Rev 34(4):369–376 **(in Chinese)**
Cui ZJ, Gao QZ, Liu GN, Pan BT, Chen HL (1996) Planation surfaces, palaeokarst and uplift of Xizang (Tibet) Plateau. Sci China (Series D) 39(4):391–400
Cui P, Zhu Y, Han Y, Chen XQ, Zhuang JQ (2009) The 12 May Wenchuan earthquake-induced landslide lakes: distribution and preliminary risk evaluation. Landslides 6:209–223
Cui P, Chao D, Zhuang JQ, You Y, Chen XQ, Scott KM (2012) Landslide-dammed lake at Tangjiashan, Sichuan province, China (triggered by the Wenchuan earthquake, May 12, 2008): risk assessment, mitigation strategy, and lesson learned. Environ Earth Sci 65:1055–1065
Cui, Z.J, Li, C.C., Chen, J., (2013). Diamicton and environment: outburst deposit. Hebei: Hebei Science and Technology Press, 466–478 (in Chinese with English abstract)
Cutler PM, Colgan PM, Mickelson DM (2002) Sedimetologic evidence for outburst floods from the Laurentide Ice Sheet margin in Wisconsin, USA: implications for tunnel–channel formation. Quat Int 90:23–40
Dai FC, Lee CF, Deng JH, Tham LG (2005) The 1786 earthquake-triggered landslide dam and subsequent dam-breakflood on the Dadu River, southwestern China. Geomorphology 65:205–221
Ermini L, Casagli N (2003) Prediction of the behaviour of landslide dams using a geomorphological dimensionless index. Earth Surf Process Landf 28:31–47
Flint R, Sanders J, Rodgers J (1960) Diamictite, a substitute term for symmictite. Geol Soc Am Bull 71(12):1809–1810
Guo XH, Sun Z, Lai ZP, Lu YD, Li XL (2016) Optical dating of landslide-dammed lake deposits in the upper Yellow River, Qinghai-Tibetan Plateau, China. Quat Int 392:233–238
Hanson MA, Lian OB, Clague JJ (2012) The sequence and timing of large late Pleistocene floods from glacial Lake Missoula. Quat Sci Rev 31:67–81
Hermanns RL, Niedermann S, Ivy-Ochs S, Kubik PW (2004) Rock avalanching into a landslide-dammed lake causing multiple dam failure in Las Conchas valley (NW Argentina)—evidence from surface exposure dating and stratigraphic analyses. Landslides 1:113–122
Hodell DA, Brenner M, Kanfoush SL, Curtis JH, Stoner JS, Song XL, Wu Y, Whitmore TJ (1999) Paleoclimate of southwestern China for the past 50,000 yr inferred from lake sediment records. Quat Res 52:369–380
Jibson RW, Prentice CS, Borissoff BA, Rogozhin EA, Langer CL (1994) Some observations of landslides triggered by the 29 April 1991 Racha earthquake, Republic of Georgia. Bull Seismol Soc Am 84:964–973
Kataoka KS (2011) Geomorphic and sedimentary evidence of a gigantic outburst flood from Towada caldera after the 15ka Towada-Hachinohe ignimbrite eruption, northeast Japan. Geomorphology 125:11–26
Kataoka KS, Urabe A, Manville V, Kajiyama A (2008) Breakoutflood from an ignimbrite-dammed valley after the 5 ka Numazawako eruption, northeast Japan. Geol Soc Am Bull 120:1233–1247
Keefer DK (1984) Landslides caused by earthquakes. Bull Geol Soc Am 95:406–421
Kehew AE, Lord ML (1986) Origin and large–scale erosional features of glacial–lake spillways in the northern Great Plains. Geol Soc Am Bull 97:162–177
Khazai B, Sitar N (2004) Evaluation of factors controlling earthquake-induced landslides caused by Chi-Chi earthquake and comparison with the Northridge and Loma Prieta events. Eng Geol 71:79–95

Korup O (2002) Recent research on landslide dams—a literature review with special attention to New Zealand. Prog Phys Geogr 26:206–235
Korup O, Montgomery DR (2008) Tibetan Plateau river incision inhibited by glacial stabilization of the Tsangpo Gorge. Nature 455(7214):786–789
Korup O, Tweed F (2007) Ice, moraine, and landslide dams in mountainous terrain. Quat Sci Rev 26:3406–3422
Korup O, Görüm T, Hayakawa Y (2012) Without power? Landslide inventories in the face of climate change. Earth Surf Process Landf 37:92–99
Li JJ, Fang XM (1998) Tibetan plateau uplift and environmental change. Chin Sci Bull 43(15):1569–1574
Li, T.C., Schuster, R.L., Wu, J.S., 1986. Landslide dams in south-central China. In: Schuster, R.L., ed., Landslide dams—processes, risk, and mitigation: American Society of Civil Engineers Geotechnical Special Publication 3, p. 146–162
Liu WM, Lai ZP, Hu KH, Ge YG, Cui P, Zhang XG, Liu F (2015) Age and extent of a giant glacial-dammed lake at Yarlung Tsangpo gorge in the Tibetan Plateau. Geomorphology 246:370–376
Lord ML, Kehew AE (1987) Sedimentology and paleohydrology of glacial–lake outburst deposits in southeastern Saskatchewan and northwestern North Dakota. Geol Soc Am Bull 99:663–673
Lowe DR (1975) Water escape structures in coarse-grained sediments. Sedimentology 22:157–204
Mills PC (1983) Genesis and diagnostic value of soft-sediment deformation structures—a review. Sediment Geol 35:83–104
Murray AS, Wintle AG (2000) Luminescence dating of quartz using an improved single aliquot regenerative-dose protocol. Radiat Meas 32:57–73
Obermeier SF (1996) Use of liquefaction-induced features for paleoseismic analysis—an overview of how seismic liquefaction features can be distinguished from other features and how their regional distribution and properties of source sediment can be used to infer the location and strength of Holocene paleo-earthquakes. Eng Geol 44:1–76
Owen G (1996) Experimental soft-sediment deformation: structures formed by the liquefaction of unconsolidated sands and some ancient examples. Sedimentology 43:279–293
Prescott JR, Stephan LG (1982) The contribution of cosmic radiation to the environmental dose of thermolumincence dating: latitude, altitude and depth dependencies. PACT 6:17–25
Regmi NR, Giardino JR, Vitek JD (2014) Characteristics of landslides in western Colorado, USA. Landslides 11(4):589–603
Reid LM, Page MJ (2003) Magnitude and frequency of landsliding in a large New Zealand catchment. Geomorphology 49:71–88
Reneau SL, Dethier DP (1996) Late Pleistocene landslide–dammed lakes along the Rio Grande, White Rock Canyon, New Mexico. Geol Soc Am Bull 108(11):1492–1507
RGSTY (Regional Geological Survey Team of the Yunnan Bureau of Geology and Mineral Resources). 1982. Regional geological survey report of the People's Republic of China: Guxue image (scale: 1:200000), People's Republic of China
Schuster RL, Nieto AS, O'ouke TD, Crespo E, Plaza-Nieto G (1996) Mass wasting triggered by the 5 March 1987 Ecuador earthquakes. Eng Geol 42:1–23
Scott, K.M., Gravlee, G.C., 1968. Flood and surge on the Rubicon River, California—hydrology, hydraulics and boulder transport: U.S. Geological Survey Professional Paper 422–M, 40 P
Soeters, R.S. and Van Westen, C.J., 1996. Slope instability recognition, analysis and zonation. National Academy Press, 129–177
Stuiver M, Reimer PJ (1993) Extended ^{14}C data base and revised CALIB 3.0 ^{14}C age calibration program. Radiocarbon 35:215–230
Trauth MH, Strecker MR (1999) Formation of landslide-dammed lakes during a wet period between 40,000 and 25,000 yr B.P. in northwestern Argentina. Palaeogeogr, Paleoclimatol, Paleoecol 153:277–287
Van Gorp W, Veldkamp A, Temme AJAM, Maddy D, Demir T, Van der Schriek T, Reimann T, Wallinga J, Wijbrans J, Schoorl JM (2013) Fluvial response to Holocene volcanic damming and breaching in the Gediz and Geren rivers, western Turkey. Geomorphology 201:430–448
Walder JS, Costa JE (1996) Outburst floods from glacier-dammed lakes: the effect of mode of lake drainage on flood magnitude. Earth Surf Process Landf 21:701–723
Wang PF, Chen J, Dai FC, Long W, Xu C, Sun JM, Cui ZJ (2014) Chronology of relict lake deposits around the Suwalong paleolandslide in the upper Jinsha River, SE Tibetan Plateau: implications to Holocene tectonic perturbations. Geomorphology 217:203–213
Waythomas CF (2001) Formation and failure of volcanic debris dams in the Chakachatna River valley associated with eruptions of the Spurr volcanic complex, Alaska. Geomorphology 39:111–129
Wen XZ, Ma SL, Xu XW, He YN (2008) Historical pattern and behavior of earthquake ruptures along the eastern boundary of the Sichuan-Yunnan faluted-block, southwestern China. Phys Earth Planet Inter 168:16–36
Wilford DJ, Sakals ME, Innes JL, Sidle RC, Bergerud WA (2004) Recognition of debris flow, debris flood and flood hazard through watershed morphometrics. Landslides 1:61–66
Wu XG, Cai CX (1992) The neotectonic activity along the central segment of Jinshajiang fault zone and the epicentral determination of Batang M 6.5 earthquake. J Seismol Res 15(4):401–410 **(in Chinese with English abstract)**
Wu QL, Zhao ZJ, Liu L, Granger DE, Wang H, Cohen DJ, Wu XH, Ye ML, Bar-Yosef O, Lu B, Zhang J, Zhang PZ, Yuan DY, Qi WY, Cai LH, Bai SB (2016) Outburst flood at 1920 BCE supports historicity of China's great flood and the Xia dynasty. Science 353(6299):579–582
Xu XW, Zhang PZ, Wen XZ, Qin ZL, Chen GH, Zhu AL (2005) Features of active tectonics and recurrence behaviors of strong earthquakes in the western Sichuan Province and its adjacent regions. Seismol Geol 27(3):446–461 **(in Chinese with English abstracts)**
Zhang YS, Zhao XT, Lan HX, Xiong TY (2011) A Pleistocene landslide-dammed lake, Jinsha River, Yunnan, China. Quat Int 233:72–80

J. Chen (✉) · S. Wu · J. Ma
School of Engineering and Technology,
China University of Geosciences Beijing,
Beijing, 100083, China
Email: jianchen@cugb.edu.cn

W. Zhou
Department of Geology and Geological Engineering,
Colorado School of Mines,
Golden, CO 80401, USA

Z. Cui
College of Urban and Environmental Sciences,
Peking University,
Beijing, 100871, China

W. Li
China Institute of Water Resources and Hydropower Research,
Beijing, 100038, China